

CPW-Fed Ultra-Wideband Dual-Sense Circularly Polarized Slot Antenna

Amit Birwal^{1, *}, Sanjeev Singh², Binod Kumar Kanaujia³, and Sachin Kumar⁴

Abstract—The paper presents a new coplanar waveguide (CPW)-fed ultra-wideband (UWB) dual circularly polarized (CP) slot antenna. For realizing UWB, a wide slot is introduced in the ground plane of the proposed antenna. The circular polarization is achieved by introducing a semi-circular stub in the square ground plane. The antenna contains two symmetrical CPW-fed ports at left and right edges to generate dual circular polarization. The evolution steps of the proposed CP antenna are presented, and antenna parameters are optimized to obtain the desired level of isolation, return loss, and axial ratio bandwidth (ARBW). The measured impedance bandwidth ($S_{11} \leq -10$ dB) of the antenna is 13.5 GHz (2.5–16 GHz); 3-dB ARBW is 75.23% (2.67–5.89 GHz); and isolation greater than 17 dB is obtained in the CP band. The designed dual feed CP antenna has low profile, light weight, compact size, and could be suitable for polarization diversity applications for reducing the effect of multipath fading.

1. INTRODUCTION

Wireless communication technology is considered one of the most rapidly growing industrial markets, where antenna with circular polarization has gained considerable attention in the last few years. In contrast to linearly polarized (LP) structures, circularly polarized (CP) antennas have many advantages and are widely used for contemporary wireless applications to reduce the effect of multipath fading and polarization losses between transmitting and receiving antennas [1]. Moreover, in order to obtain a high transmission rate, large system capacity and to eliminate polarization mismatch losses, ultra-wideband (UWB) CP antennas are required [2]. A conventional method to generate CP radiation entails excitation of two orthogonal current modes of equal magnitude and quadrature phase difference. An alteration in radiator or ground plane will account for this quadrature phase shift in the case of single feed CP antennas. However, the single feed CP antennas have narrow axial ratio bandwidth (ARBW), and to realize a wide ARBW, dual feed CP antennas are preferred.

Recently, various single and dual feed CP antenna configurations have been reported for mobile communication, radio frequency identification (RFID), satellite communication, worldwide interoperability for microwave access (Wi-MAX), wireless local area networks (WLAN), and wireless power transmission (WPT) applications [3–5]. Most of the antennas reported in the literature generate only one type of polarization, either left-hand circular polarization (LHCP) or right-hand circular polarization (RHCP) [1–5]; however, for polarization diversity systems a dual polarization is needed [6, 7]. A single feed patch antenna with two orthogonal slots and two pin diodes was proposed in [8], and by controlling the bias voltage of the pin diodes, the desired LHCP/RHCP pattern can be

Received 20 May 2019, Accepted 23 July 2019, Scheduled 1 August 2019

* Corresponding author: Amit Birwal (amit.birwal@south.du.ac.in).

¹ Department of Electronic Science, University of Delhi South Campus, New Delhi 110022, India. ² Institute of Informatics and Communication, University of Delhi South Campus, New Delhi 110022, India. ³ School of Computational and Integrative Sciences, Jawaharlal Nehru University, New Delhi 110067, India. ⁴ School of Electronics Engineering, Kyungpook National University, Daegu 41566, Republic of Korea.

obtained. The antenna reported in [9] was composed of a square slot, a T-shaped metal strip, and two microstrip T-junctions, and for generating RHCP/LHCP patterns simultaneously, two $50\ \Omega$ microstrip lines were used. In microstrip line-fed antennas, it is difficult to preserve the metallic layer alignment on both sides of the printed circuit board (PCB). Therefore, smooth device integration is not possible in the case of monolithic microwave integrated circuits (MMICs) [10]. A coplanar waveguide (CPW)-fed antenna supports easy device integration and wide impedance bandwidth by using a single metallic layer on one side of the substrate. A CPW-fed square slot CP antenna with more than 18% 3-dB ARBW was presented [11]. In [12], a CP antenna composed of two T-shaped feeding structures and an inverted-L grounded strip was proposed, which can generate both LHCP and RHCP waves. A CPW-fed two-port square slot antenna with dual-band and dual-sense polarization was presented [13]. In [14], a CPW-fed slot antenna loaded with two spiral slots in the ground surface was reported for dual-sense circular polarization. A dual-band dual-sense antenna composed of an asymmetric rectangular slot and parasitic radiators excited through F-shaped feed line was reported [15]. A U-shaped microstrip line-fed square slot antenna consisting of parasitic and antipodal Y-shaped metal strips to realize CP operation was proposed [16]. In [17], a CPW-fed slot antenna composed of a C-shaped grounded strip for dual-band CP operation was presented. A CPW-fed antenna composed of two parasitic patches and an asymmetric feed line for dual frequency operation was reported [18]. A CPW-fed slot antenna consisting of inverted L-shaped and asymmetric U-shaped slots for dual-frequency and dual circular polarization was proposed [19]. A CPW-fed wideband CP monopole antenna composed of an asymmetric ground plane and a square-ring with an opening at the lower edge was reported [20]. However, the above-reported CP antennas have smaller ARBW, relatively large size, limited resonating bands, complicated geometry with decoupling elements, and external feeding circuitry. Therefore, a compact CPW-fed UWB CP antenna with wide ARBW and dual circular polarization is desired for modern high data rate wireless communication systems.

In this article, a dual-port CPW-fed CP antenna is presented. The projected CP antenna consists of two P-shaped radiators, and by introducing wide slot, semi-circular and triangular structures in the ground plane, ultra-wide impedance bandwidth and ARBW are realized. The proposed CP antenna can generate RHCP and LHCP waves simultaneously. The proposed antenna is designed and optimized with commercially available CST microwave studio tool. The antenna is fabricated, and experimental results are found in good agreement with the simulated ones. The proposed UWB antenna features a small size and broad 3-dB ARBW as compared to the antennas reported in the literature [11–20]. The antenna is suitable for polarization diversity and UWB communication systems.

2. ANTENNA CONFIGURATION

The geometry of the proposed dual-port CP antenna is shown in Fig. 1. The antenna contains two identical P-shaped radiators excited through CPW feed lines of $50\ \Omega$. In Fig. 1(a), one semi-circular and two triangular stubs are integrated at the center and edges of the square ground plane to achieve circular polarization and high isolation between the radiating elements. The spacing between the feed line and the ground plane is optimized to obtain a good impedance matching in the entire UWB. Fig. 1(b) illustrates the fabricated prototype antenna. The antenna is printed on one side of an FR-4 dielectric substrate ($\epsilon_r = 4.4$ and $\tan \delta = 0.04$) with overall dimensions of $48 \times 48 \times 1.5\ \text{mm}^3$. The designing parameters of the proposed antenna are shown in Table 1.

To better understand the designing process, evolution steps of the proposed antenna are shown in Fig. 2. The configuration (Ant. 1) shown in Fig. 2(a) is a typical two-port CPW-fed square-shaped antenna. A wide square slot is introduced in the antenna geometry to obtain wide impedance bandwidth. In Figs. 3(a), (b), and (c), the respective return loss (S_{11}), isolation (S_{21}), and axial ratio are compared during the evolution stages of the proposed antenna. Ant. 1 offers only one operating band (at around 15 GHz) with no CP radiations in this band. In the next step as shown in Fig. 2(b), a semi-circular stub (Ant. 2) is introduced in the square ground plane of Ant. 1. By introducing a semi-circular stub in the ground plane, circular polarization is obtained in the lower frequency region (around 2.9–3.5 GHz). In Fig. 2(c), two P-shaped radiators are designed (Ant. 3) to improve the impedance bandwidth of the proposed antenna. A better impedance matching is provided by the P-shaped radiators that help in obtaining UWB. In Fig. 2(d), to broaden the ARBW, two similar triangular stubs are added (Ant. 4) in

Table 1. Dimensions of the proposed two-port CP antenna.

| Parameter | Value (mm) | Parameter | Value (mm) |
|-----------|------------|-----------|------------|
| L | 48 | W_2 | 35 |
| W | 48 | R_1 | 4.5 |
| L_1 | 9 | R_2 | 10.2 |
| L_2 | 5.7 | S | 10 |
| L_3 | 9.7 | g | 0.8 |
| W_1 | 6.5 | | |

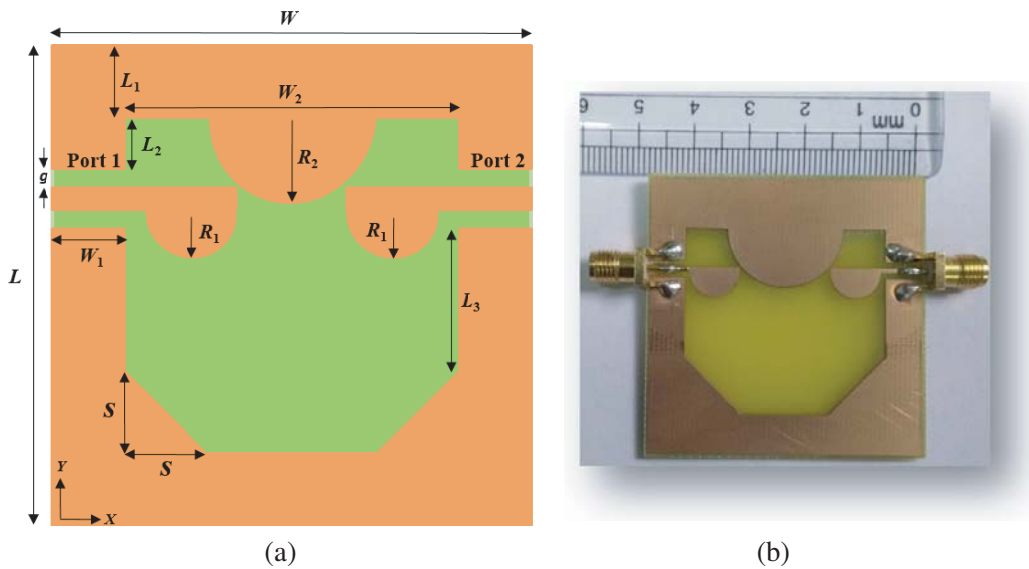


Figure 1. Geometry of the proposed dual-port CP antenna. (a) Top view, (b) fabricated prototype.

the ground plane of the antenna. The triangular stubs influence current distribution on the surface of the antenna, and consequently, an improved axial ratio is obtained. It is noticed that the proposed antenna provides a 3-dB ARBW of 3.3 GHz (2.6–5.9 GHz), and port isolation greater than 17 dB is obtained in the CP band.

3. PARAMETRIC ANALYSIS

The parametric analysis of the proposed CP antenna is performed by varying different design parameters and observing their effect on S_{11} , S_{21} , and axial ratio. For this study, one of the design parameters is changed, while keeping other dimensions fixed, and its impact on the performance of the antenna is noticed. Performance of the antenna is analysed for different values of R_1 , R_2 , and S , when excitation is applied at port-1, and port-2 is matched to 50Ω termination. Since the proposed structure is symmetrical with identical radiating elements, the antenna performance is studied at port-1 only.

3.1. Radius R_1 of P-Shaped Radiator

Figures 4(a), (b), and (c) show respective S_{11} , S_{21} , and axial ratio response of the antenna by varying semi-circle radius R_1 of P-shaped radiator. It can be observed from Fig. 4(a) that by increasing radius R_1 , an improvement in impedance matching is achieved, which results in broad impedance bandwidth. In Fig. 4(b), the mutual coupling effect between port-1 and port-2 is shown. The radius R_1 does not affect S_{21} much in the higher frequency range. But at lower frequencies, a reduction in S_{21} is noticed

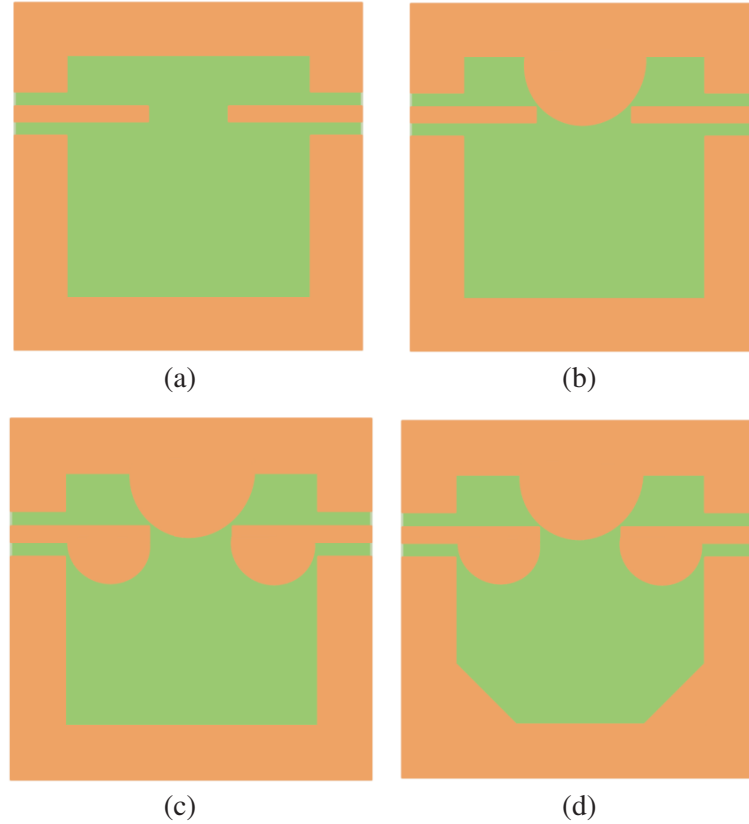


Figure 2. Evolution steps of the proposed CP antenna. (a) Ant. 1, (b) Ant. 2, (c) Ant. 3, (d) Ant. 4.

by increasing R_1 . As illustrated in Fig. 4(c), a significant change in axial ratio is seen by reducing the radius R_1 . Considering the matching and 3-dB ARBW, the R_1 is chosen to be 4.5 mm.

3.2. Radius R_2 of Semi-Circular Stub

Figures 5(a), (b), and (c) display S_{11} , S_{21} , and axial ratio curves by varying radius R_2 of the semi-circular stub, respectively. It is noticed that the radius R_2 significantly impacts the ARBW of the antenna. With increasing R_2 , the gap between the P-shaped radiator and semi-circular stub decreases, which directly influences the antenna coupling. This further impacts the distribution of current at higher operating frequencies, and consequently, an improved ARBW is observed. Increasing R_2 has a minor impact on S_{11} and S_{21} . For antenna designing, R_2 is optimized to be 10.2 mm.

3.3. Side S of Triangular Stub

Figures 6(a), (b), and (c) depict the variations of S_{11} , S_{21} , and axial ratio by changing the triangular stub side S , respectively. As seen from Figs. 2(c) and (d) (in the evolution steps), the triangular stub significantly improves the ARBW of the proposed antenna. It is observed that with increasing S from 8 to 10 mm, a better 3-dB ARBW is achieved, while a further increment in the value of S results in narrow ARBW. S has a minor impact on S_{11} and S_{21} . For antenna designing, the final optimized value of S is selected to be 10 mm.

4. CIRCULAR POLARIZATION MECHANISM

Figure 7 shows the mechanism to demonstrate circular polarization in the proposed two-port antenna. CP radiation can be realized when two orthogonal resonant modes are generated with equal amplitude

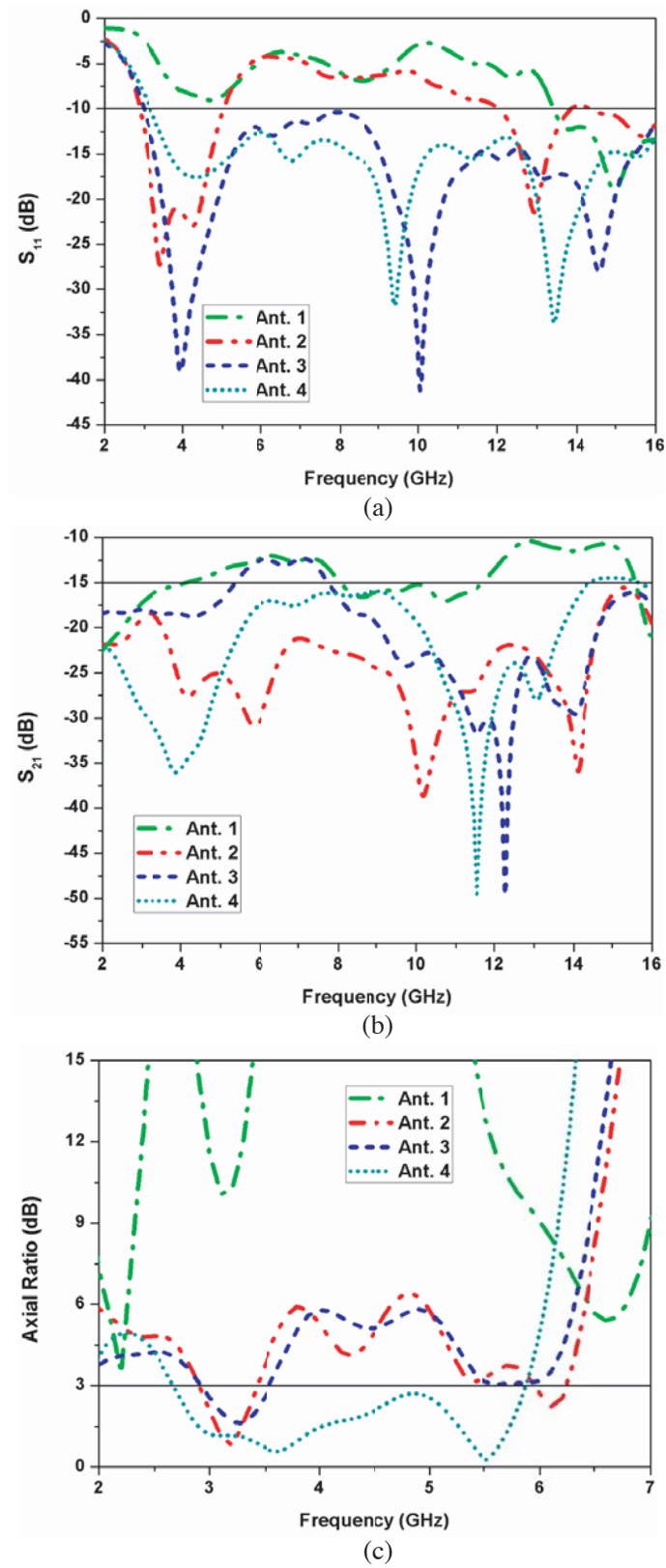


Figure 3. Comparison of antenna performance. (a) Magnitude of S_{11} , (b) magnitude of S_{21} , (c) axial ratio.

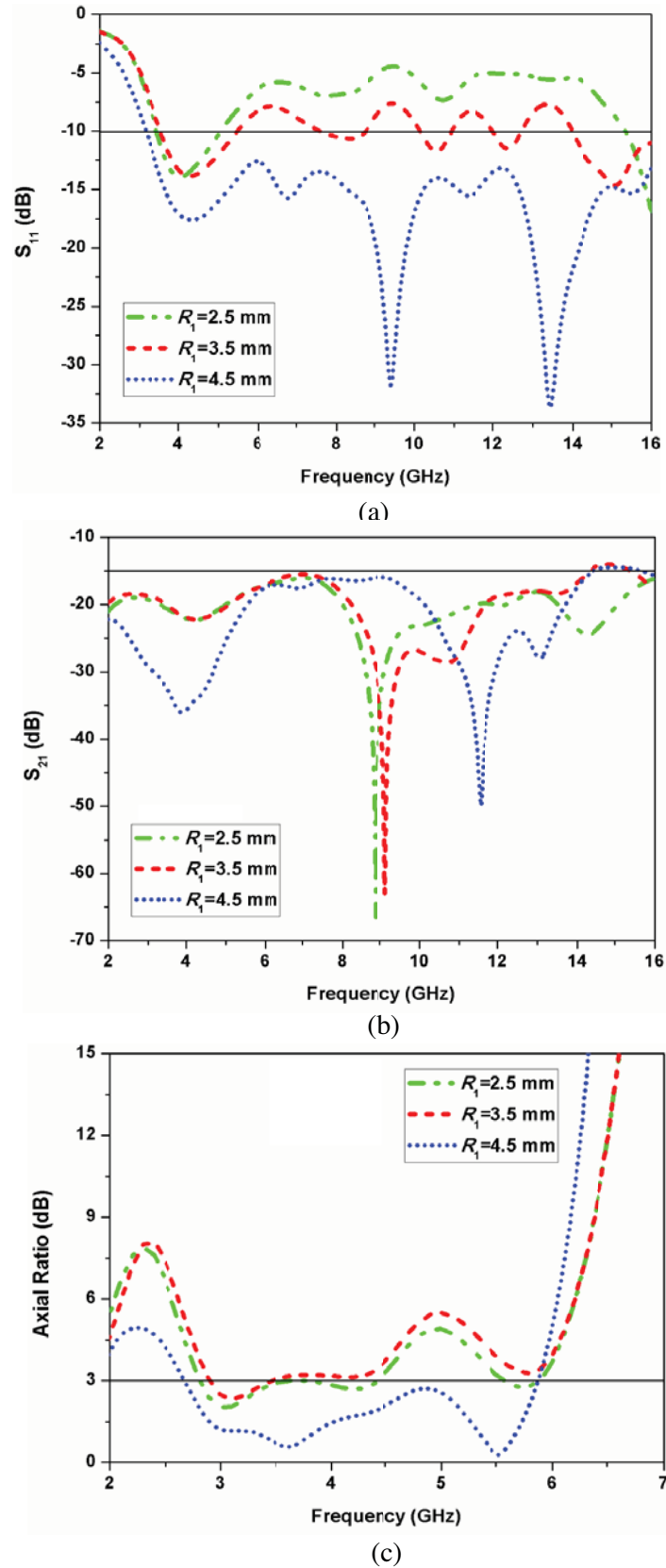


Figure 4. Effect of radius R_1 on (a) magnitude of S_{11} , (b) magnitude of S_{21} , (c) axial ratio.

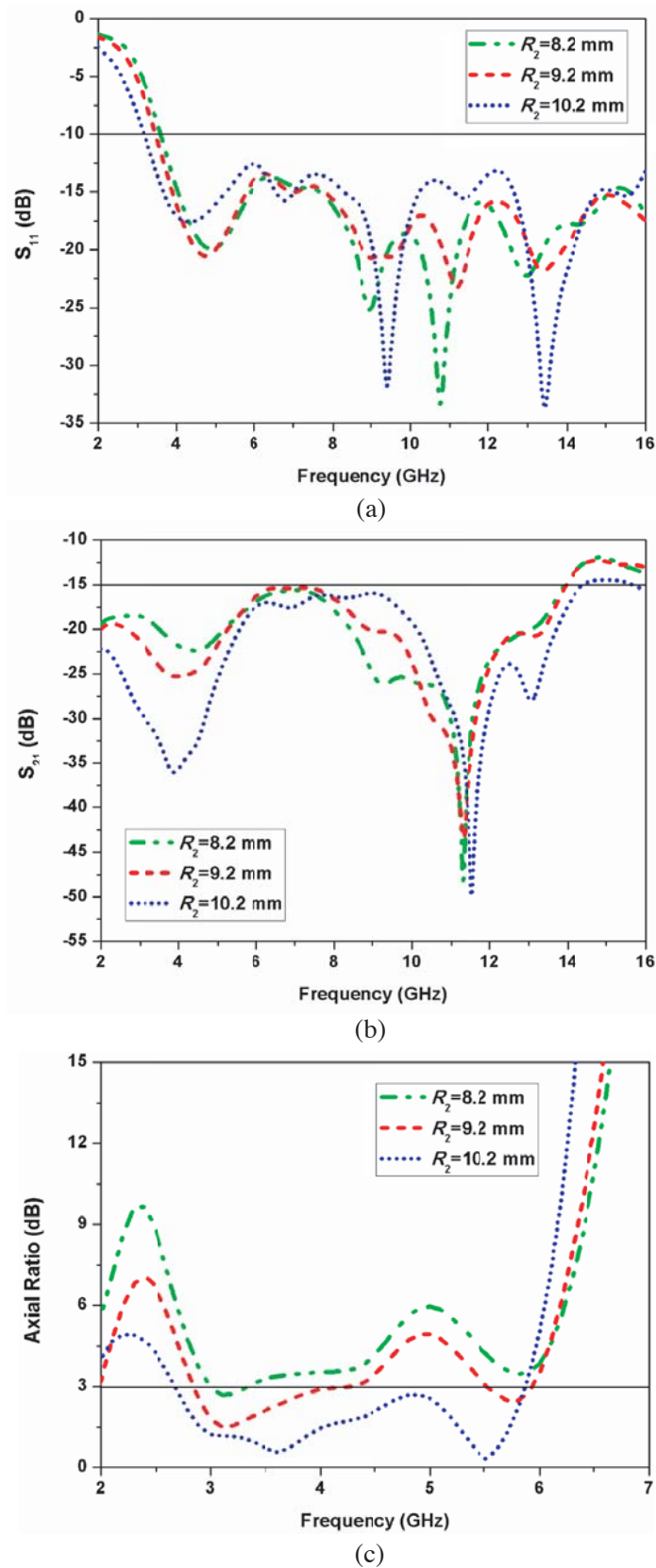


Figure 5. Effect of radius R_2 on (a) magnitude of S_{11} , (b) magnitude of S_{21} , (c) axial ratio.

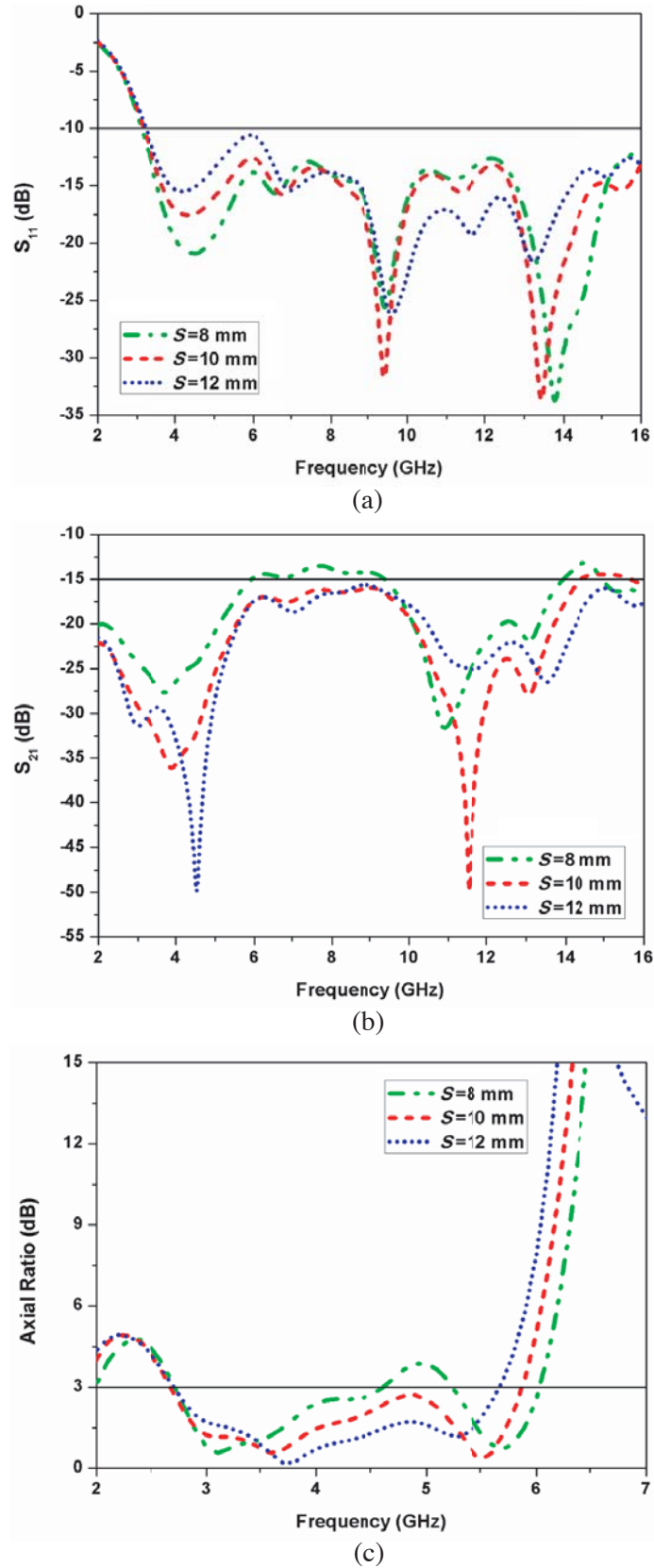


Figure 6. Effect of length S on (a) magnitude of S_{11} , (b) magnitude of S_{21} , (c) axial ratio.

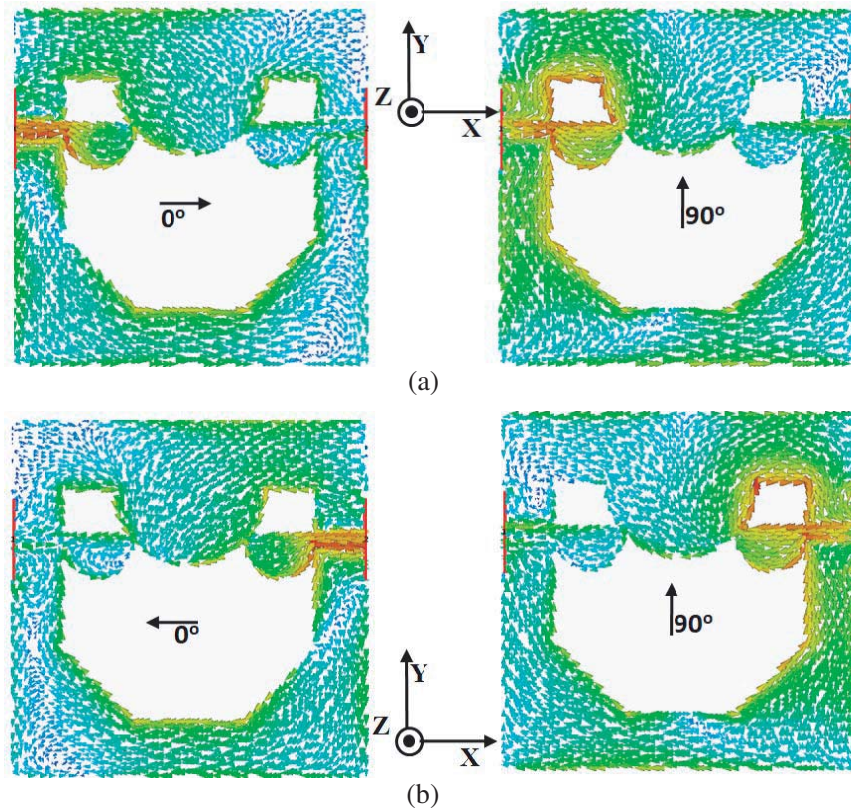


Figure 7. Surface current at 3.5 GHz when (a) port-1 is excited, (b) port-2 is excited.

and 90° phase difference. When port-1 is excited, port-2 is terminated with a $50\ \Omega$ matched load. Fig. 7(a) displays the current distribution (at 3.5 GHz) when a 0° phase signal is applied to port-1, and the dominant vector currents are seen along $+X$ -direction. Likewise, when a signal with a 90° phase is applied to port-1, the dominant vector current flows along $+Y$ -direction. The same phenomenon happens when signals with 180° and 270° phases are applied to port-1. In this case, the dominant current has equal magnitudes but opposite phases with respect to those at 0° and 90° . As seen from the $+Z$ -direction, it appears that the rotation of the surface current is in a counterclockwise direction, which results in RHCP radiation.

Similarly, in Fig. 7(b), when 0° and 90° phase signals are applied to port-2, the dominant vector current moves from $-X$ - to $+Y$ -direction. Here, as seen from $+Z$ -direction, the rotation of the surface current is in a clockwise direction, hence LHCP radiation is observed. The dual circular polarization can be achieved by feeding port-1 and port-2 of the proposed antenna simultaneously.

5. RESULTS AND DISCUSSION

The antenna is fabricated with the help of the photolithography method, and measurements are performed using Keysight N5227A vector network analyzer. Fig. 1(b) displays the fabricated prototype of the proposed dual-port CP antenna. The simulated and measured reflection coefficients and port isolation of the proposed CP antenna are shown in Fig. 8. The measured impedance bandwidth of the proposed antenna extends from 2.5 to 16 GHz (13.5 GHz) covering the complete UWB. The measured isolation between the two ports is greater than 17 dB. Fig. 9 shows simulated and measured gain and axial ratio curves of the proposed antenna. It is found that the antenna's measured 3-dB ARBW is about 75.23% (2.67–5.89 GHz), and the peak gain is 2.65 dBi within the CP bandwidth. The simulated and measured radiation patterns at 3.5 GHz in both XZ - and YZ -planes are shown in Figs. 10(a) and (b) for port-1 and -2, respectively. The proposed antenna generates both RHCP and LHCP waves (in

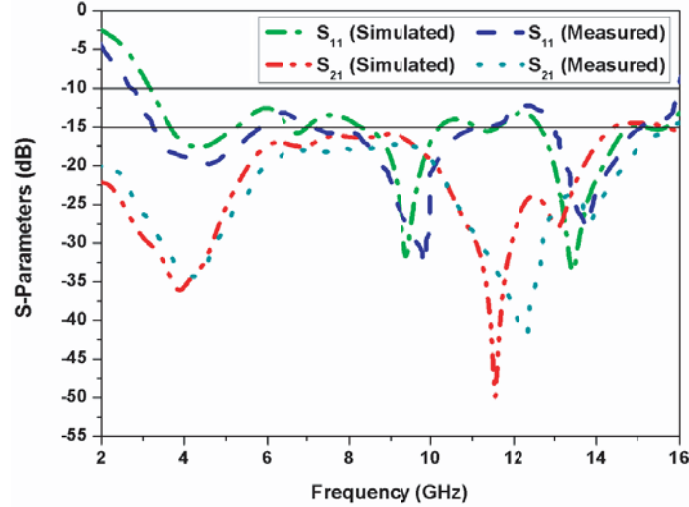


Figure 8. Simulated and measured S -parameters of the proposed CP antenna.

Table 2. Comparison of proposed CP antenna with other reported CP antennas.

| Ref. | Size (mm ²) | −10 dB Impedance Bandwidth (GHz) | CP Band (GHz) | 3-dB ARBW (GHz)/% | Polarization |
|-----------|-------------------------|----------------------------------|--------------------------|--------------------------|--------------|
| [12] | 60 × 60 | 2–4.76 | 2–3.7 | 1.7/59.65 | RHCP/LHCP |
| [13] | 70 × 70 | 1.4–4 | 1.48–1.75, 3.4–3.57 | 0.27/16.72, 0.17/4.7 | RHCP/LHCP |
| [14] | 70 × 70 | 1.54–1.68, 1.96–2.47 | 1.54–1.675, 2.02–2.45 | 0.315/8.4, 0.43/19.24 | RHCP/LHCP |
| [15] | 63.5 × 55 | 1.57–2.04, 2.87–3.47 | 1.6–2, 3.15–3.5 | 0.4/22.22, 0.35/10.53 | RHCP/LHCP |
| [16] | 63 × 75 | 1.81–3.83 | 2.2–2.9, 3.4–3.65 | 0.7/27.45, 0.25/7.1 | RHCP/LHCP |
| [17] | 70 × 70 | 1.01–3.33 | 1.41–1.96, 2.45–2.59 | 0.55/32.35, 0.14/5.6 | RHCP/LHCP |
| [18] | 70 × 70 | 1.17–2.24, 2.55–5.77 | 1.25–2.24, 2.77–2.86 | 0.99/57.09, 0.09/3.24 | RHCP/LHCP |
| [19] | 60 × 60 | 2.51–3.72, 4.83–6.37 | 2.50–3.65, 5.02–5.91 | 1.15/37.4, 0.89/16.3 | RHCP/LHCP |
| [20] | 90 × 100 | 0.88–3.08, 3.64–5.58 | 0.98–2.68, 3.69–5.5 | 1.7/92.9, 1.81/39.4 | RHCP/LHCP |
| This work | 48 × 48 | 2.5–16 | 2.67–5.89 | 3.22/75.23 | RHCP/LHCP |

the + Z -direction) at the same frequency.

Table 2 shows the comparison of various characteristics of the proposed CP antenna with previously reported CP antenna structures. The designs presented in [14–18] are composed of single CPW-fed radiator to achieve dual CP operation. The dual-band dual-sense polarization based antenna structures reported in [19, 20] are composed of an L-shaped radiating patch and modified ground plane. Since only a few studies are available on UWB dual-sense CP antennas, Table 2 is updated with [12, 13] as the

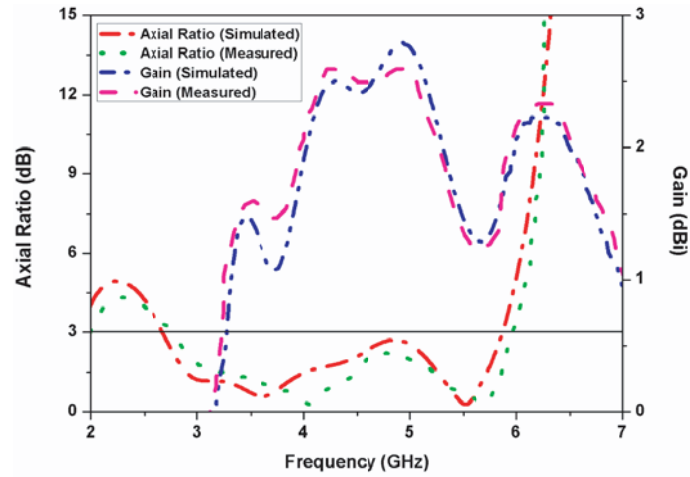


Figure 9. Simulated and measured axial ratio/gain of the proposed CP antenna.

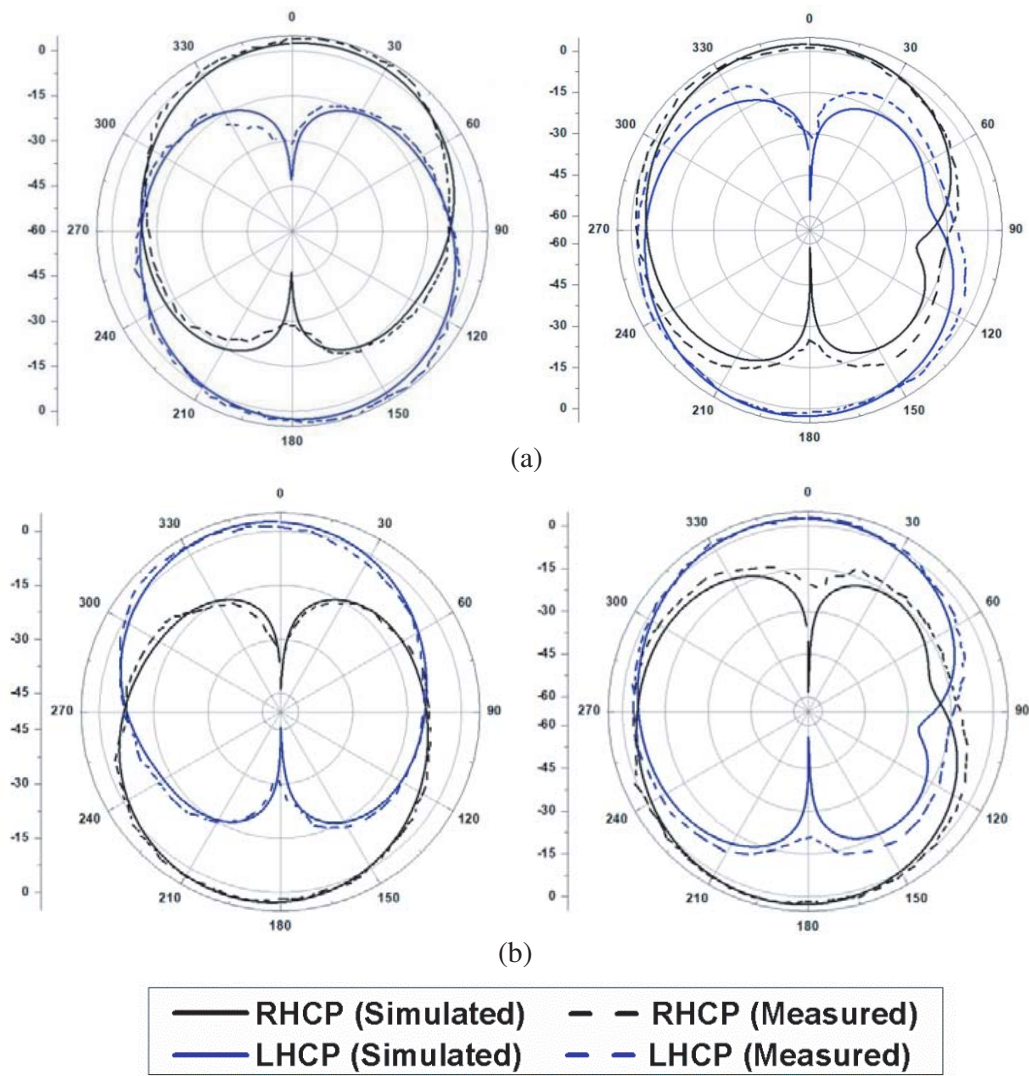


Figure 10. Simulated and measured radiation patterns at 3.5 GHz when excitation is at (a) port-1, (b) port-2.

designs mentioned here consisting of a two-port CPW-fed antenna to generate dual circular polarization. However, the antennas mentioned here [12–20] have relatively large size and narrow impedance and CP bands.

6. CONCLUSION

In this paper, a planar CPW-fed CP antenna with UWB response is presented. By introducing semi-circular and triangular stubs in the square ground plane of the proposed antenna, a broad impedance and CP bandwidth are achieved. The antenna is fabricated on an FR-4 substrate, and measured results are found in close proximity with the simulated results. A measured 3-dB ARBW of 75.23% (2.67–5.89 GHz), isolation greater than 17 dB, and peak gain of 2.65 dBi are obtained within the CP band of the proposed antenna. Simultaneously, the antenna can generate both RHCP and LHCP waves without changing the operating frequency of the ports. The proposed UWB CP antenna may be useful for high-speed data transmission, where polarization diversity is required to improve link reliability and capacity of the wireless system, without increasing the transmitted power or channel bandwidth.

REFERENCES

1. Kumar, S., B. K. Kanaujia, A. Sharma, M. K. Khandelwal, and A. K. Gautam, “Single feed cross slot loaded compact circularly polarized microstrip antenna for indoor WLAN applications,” *Microw. Opt. Technol. Lett.*, Vol. 56, No. 6, 1313–1317, 2014.
2. Xu, R., J. Li, J. Liu, S. G. Zhou, and K. Wei, “UWB circularly polarised slot antenna with modified ground plane and L-shaped radiator,” *Electron. Lett.*, Vol. 54, No. 15, 918–920, 2018.
3. Srivastava, K., A. Kumar, B. K. Kanaujia, S. Dwari, and S. Kumar, “Low profile coupling feed circularly polarized antennas for WLAN applications,” *Int. J. RF Microw. Comput. Aided Eng.*, Vol. 29, No. 2, e21525, 2019.
4. Khandelwal, M. K., S. Kumar, and B. K. Kanaujia, “Design, modeling and analysis of dual-feed defected ground microstrip patch antenna with wide axial ratio bandwidth,” *J. Comput. Electron.*, Vol. 17, No. 3, 1019–1028, 2018.
5. Singh, N., B. K. Kanaujia, M. T. Beg, Mainuddin, T. Khan, and S. Kumar, “A dual polarized multiband rectenna for RF energy harvesting,” *AEU-Int. J. Electron. Commun.*, Vol. 93, 123–131, 2018.
6. Srivastava, K., A. Kumar, B. K. Kanaujia, S. Dwari, and S. Kumar, “Low profile single feed monopole antenna for quad-band circularly polarised applications,” *Int. J. Electron.*, Vol. 106, No. 2, 318–331, 2019.
7. Saxena, S., B. K. Kanaujia, S. Dwari, S. Kumar, and R. Tiwari, “A compact dual-polarized MIMO antenna with distinct diversity performance for UWB applications,” *IEEE Antennas Wireless Propag. Lett.*, Vol. 16, 3096–3099, 2017.
8. Yang, F. and Y. Rahmat-Samii, “A reconfigurable patch antenna using switchable slots for circular polarization diversity,” *IEEE Microwave Wireless Compon. Lett.*, Vol. 12, No. 3, 96–98, 2002.
9. Zhao, G., L. N. Chen, and Y. C. Jiao, “Design of a broadband dual circularly polarized square slot antenna,” *Microw. Opt. Technol. Lett.*, Vol. 50, No. 10, 2639–2642, 2008.
10. Gupta, K. C., R. Garg, and I. J. Bahl, *Microstrip Lines and Slot Lines*, 2nd Edition, Artech House, Norwood, MA, 1996.
11. Sze, J. Y., K. L. Wong, and C. C. Huang, “Coplanar waveguide-fed square slot antenna for broadband circularly polarized radiation,” *IEEE Trans. Antennas Propag.*, Vol. 51, No. 8, 2141–2144, 2003.
12. Saini, R. K. and S. Dwari, “A broadband dual circularly polarized square slot antenna,” *IEEE Trans. Antennas Propag.*, Vol. 64, No. 1, 290–294, 2016.
13. Saini, R. K. and S. Dwari, “Dual-band dual-sense circularly polarized square slot antenna with changeable polarization,” *Microw. Opt. Technol. Lett.*, Vol. 59, No. 4, 902–907, 2017.

14. Chen, C. and E. K. N. Yung, "Dual-band dual-sense circularly-polarized CPW-fed slot antenna with two spiral slots loaded," *IEEE Trans. Antennas Propag.*, Vol. 57, No. 6, 1829–1833, 2009.
15. Saini, R. K. and P. S. Bakariya, "Dual-band dual-sense circularly polarized asymmetric slot antenna with F-shaped feed line and parasitic elements," *Progress In Electromagnetics Research M*, Vol. 69, 185–195, 2018.
16. Saini, R. K., S. Dwari, and M. K. Mandal, "CPW-fed dual-band dual-sense circularly polarized monopole antenna," *IEEE Antennas Wireless Propag. Lett.*, Vol. 16, 2497–2500, 2017.
17. Chen, Y. Y., Y. C. Jiao, G. Zhao, F. Zhang, Z. L. Liao, and Y. Tian, "Dual-band dual-sense circularly polarized slot antenna with a C-shaped grounded strip," *IEEE Antennas Wireless Propag. Lett.*, Vol. 10, 915–918, 2011.
18. Saini, R. K., P. S. Bakariya, and P. Kumar, "Coplanar waveguide fed dual-band dual-sense circular polarized square slot antenna," *Int. J. RF Microw. Comput. Aided Eng.*, Vol. 28, No. 9, e21503, 2018.
19. Rui, X., J. Li, and K. Wei, "Dual-band dual-sense circularly polarised square slot antenna with simple structure," *Electron. Lett.*, Vol. 52, 578–580, 2016.
20. Xu, R., J. Y. Li, J. Liu, S. G. Zhou, and K. Wei, "Design of spiral slot-based dual-wideband dual-sense CP antenna," *IET Microw. Antennas Propag.*, Vol. 13, 76–81, 2018.